DENTAL MATERIALS 35 (2019) 818–824

Available online at www.sciencedirect.com

ScienceDirect

journal homepage: www.intl.elsevierhealth.com/journals/dema

# Relationship between Canal Enlargement and Fracture Load of Root Dentin Sections

*Lais S. Munari*[a,*], *Walter R. Bowles*[b], *Alex S.L. Fok*[b,c]

[a] *Department of Restorative Dentistry, Faculty of Dentistry, Newton Paiva Ferreira Cultural Institute, Rua José Cláudio Rezende, 420 - Estoril, Belo Horizonte - MG, CEP 30494-230, Belo Horizonte, MG, Brazil*

[b] *Department of Restorative Sciences, School of Dentistry, University of Minnesota, Moos Health Sciences Tower, 515 Delaware Street S.E., Minneapolis, MN, 55455, USA*

[c] *Minnesota Dental Research Center for Biomaterials and Biomechanics, School of Dentistry, University of Minnesota, Moos Health Sciences Tower, 515 Delaware Street S.E., Minneapolis, MN, 55455, USA*

ARTICLE INFO

*Article history:*
Received 6 February 2019
Accepted 13 February 2019

*Keywords:*
Vertical root fracture
endodontic instrumentation
finite element analysis

ABSTRACT

*Objective.* To investigate the effect of endodontic instrumentation on fracture susceptibility of root
dentin using experiments and stress analysis.

*Methods.* Root canals of lower premolars were enlarged with different tapers. After, teeth were cut into 2-mm sections. A metal rod of the same taper was pushed through the center of the sections using a universal test system to fracture them. The fracture load was determined from the peak load on the load-displacement curve. To determine fracture-causing stress, an axisymmetric FE model was created. An analytical solution was developed to understand the relationship between fracture load, geometrical and material parameters.

*Results.* For the same taper, increased root canal diameter did not lead to reduced fracture load. Both analytical and FE solutions showed positive linear relationship between fracture load and enlarged root canal diameter. The hoop stress was maximum at inner surface of enlarged root canal and reduced with increasing radial distance from the center. Bending of sections introduced further nonuniform stresses along the depth. Predictions for the fracture load based on the maximum hoop stress were closest to experimental values; however, account must be taken of the variation in fracture stress of dentin along the root length.

Significance Our results rejected the hypothesis that fracture load of root dentin sections reduced with endodontic instrumentation size. However, the stress distributions in whole endodontically treated teeth are more complicated. Thus, caution is necessary when using thin root sections to investigate the effect of endodontic instruments on vertical root fracture.



* Corresponding author at Rua da Mata 205 # 1806-2 Bairro Vila da Serra, 34006-086, Nova Lima, MG, Brazil
E-mail address: laismunari@hotmail.com (L.S. Munari).

https://doi.org/10.1016/j.dental.2019.02.015

## 1. Introduction

In performing endodontic treatment, dental practitioners use stainless-steel hand or rotary files to widen the root canal, removing the infected pulp tissue and dentin from within in the process [1–3]. Root canal preparation should preserve the canal path while eliminating microorganisms from the whole system [4]. While larger files remove more dentin and make canal debridement and irrigation easier [5], they can produce increased friction and stresses on the canal wall that may damage the root structure [6]. Shemesh et al. [7,8] showed that dentinal defects, such as craze lines, cracks or fractures, were introduced during root canal treatments. Fractures occur when the tensile stress in the root canal wall exceeds the remaining tensile strength of dentin [9–11]. Vertical root fractures (VRFs), occurring most often in teeth that have previously received endodontic treatment, are generally oriented in the buccal-lingual direction, extending vertically along the tooth [12]. The association of VRFs with endodontic treatment was found to be as high as 67% in molars [13]. VRFs are detrimental, requiring in most cases the extraction of these teeth [14–16]. A balance must therefore be established between sufficiently removing infected tissues and preserving the remaining tooth structure.

According to Meister et al. [17], excessive force exerted during compaction of gutta-percha is the main cause of VRFs (84% of the time). Barreto et al. [18] showed that cyclic mechanical loading also caused VRFs. Additionally, improper spreader placement can result in undesirable apical forces. Other factors such as occlusion problems, parafunctional habits and other dental treatment procedures can cause the micro-cracks to develop into VRFs [19,20].

The fracture susceptibility of a tooth is intrinsic to its external and internal morphology, the latter of which can be altered by endodontic instrumentation [21–26]. Previous studies have highlighted the value of preserving root dentin in order to maintain the structural integrity of endodontic treated teeth [21,23,24]. Root canal preparations that are conservative and rounded in shape are expected to eliminate stress concentration sites, leading to a lower incidence of micro- crack formation [27].

Finite element analysis (FEA) has been applied to studying the stress/strain distribution in dental structures under functional loadings [22,24,26]. One such study using models of the lower first molars showed that canal enlargement raised the stress concentration on the canal wall in the coronal third of the root [26]. Ricks-Williamson et al. [22], who simulated canal preparation in a central maxillary incisor under static loading, demonstrated that larger preparations could lead to higher stresses when vertical condensation forces were applied. Their results indicated that the highest stress was located between the middle and coronal thirds of the root, an area clinically observed to be prone to fracture during treatment. Lertchirakarn et al. [26], on the other hand, showed that reduced dentin thickness did not make endodontically treated teeth more prone to fracture, while altering the canal shape could relieve internal stress despite the significant loss of dentin [19]. Ossareh et al. [28] found that the resistance to VRFs after root canal preparation was influenced by the remaining dentin volume and moment of inertia of the root cross-section.

It is clear from the above discussion that root canal instrumentation that leads to different amounts of dentin loss can alter a tooth's resistance to fracture due to the creation of defects as well as changes in its stress distribution. However, the role of root instrumentation size in VRFs is still not clear [29–32]. In order to help resolve the conflicting results found for the association between endodontic instrumentation and root fractures, this study examined *in vitro* the effect of instrumentation size on the fracture susceptibility of root sections. Numerical and analytical modeling was also carried out to help explain the experimental results.

## 2. Materials and Methods

### 2.1. *Fracture of root sections*

Thirty-six extracted, single-rooted lower premolars were collected and stored in 0.05% sodium azide prior to testing. Each tooth was inspected for defects and those with root caries, multiple canals, signs of root fracture/root defects, or open apices were excluded from this study. The teeth were accessed with a Transmetal bur (Dentsply Maillefer, Tulsa, OK, USA), and size 10 K files (Dentsply Maillefer, Tulsa, OK, USA) were used to determine the canal length, with working length set at 1 mm short of the apical foramen [24]. Using an online random number generator, the teeth were randomly divided into three groups based on the instrumentation taper (.02,. 04, and .06). They were then instrumented using a crown down technique together with an Aseptico Surgimotor II torque control motor (Dents-ply, Tulsa, OK, USA) set at 350 rpm (manufacturer's recommended speed). K3 files (SybronEndo, Orange, CA, USA) were used for all three groups. The sequence of files used was: 25.12, 25.10, 25.08, 25.06, and 25.04. A 25.02 file was also used for the. 02 taper group to maintain the correct taper throughout the root canal. All the root canals were apically enlarged up to a file size of 35 K3, with a taper (.02,. 04, or. 06) depending on the group they were assigned to. NaOCl (5.25%) was delivered as an irrigant before changing the file using a Maxi Probe tip. The teeth were placed in a mold into which Integrity Temporary Crown and Bridge Material (Dentsply, Tulsa, OK, USA) was poured to create a stub for mounting onto an Isomet Low-Speed Saw (Buehler, Lake Bluff, IL, USA).

To standardize the specimens, the first 2 mm of the root apex was sectioned off. Afterwards, four 2-mm thick sections were cut off from each tooth, at a distance of 2-4 mm, 4.5-6.5 mm, 7-9 mm and 9.5-11.5 mm from the apex. The 2-mm thickness was found by a pilot study to produce the most consistent fracture results. Three separate stainless-steel rods were made to replicate the final size and taper of the instrument for each of the three groups. These rods were mounted on the crosshead of a Universal Testing System (MTS 858S, Eden Praire, MN, USA) to load the root sections by pushing them through the enlarged root canals. The root sections were placed in a holder directly below the crosshead and loaded to fracture at a constant rate of 0.2 mm/min. Fracture of the root sections could be identified by an audible cracking sound and

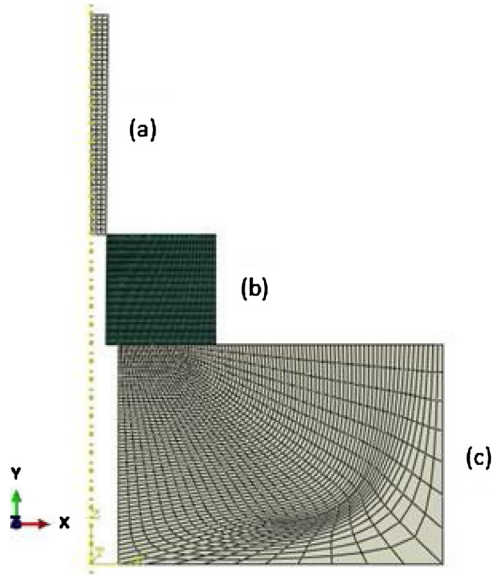


**Fig. 1 – Axisymmetric model for fracture test of root sections: (a) loading rod, (b) root section and (c) steel base.**

confirmed with a fiber optic light. The fracture load was determined from the peak load on the load-displacement curve recorded.

### 2.2. *Finite element analysis (FEA) of the root sections under loading*

A 2D, axisymmetric model consisting of the rod, root section and stainless steel base was created using the finite element software ABAQUS CAE 6.13-4 (SIMULIA, Providence, RI, MA, USA) (Fig. 1). Each component was assumed isotropic, linear-elastic and homogeneous. The elastic modulus and Poisson's ratio of the components are listed in Table 1. Loading was applied by moving the rod with a downward displacement of 4 mm through the enlarged canal of the root section. Sliding contact with a frictional coefficient of 0.3 [33] was defined between the rod and the root section as well as between the root section and the base. Both the rod and the root canal were tapered to the same angle ($\tan\theta = 0.01$, 0.02, or 0.03, Table 2). The bottom of the steel base, from which the reaction force

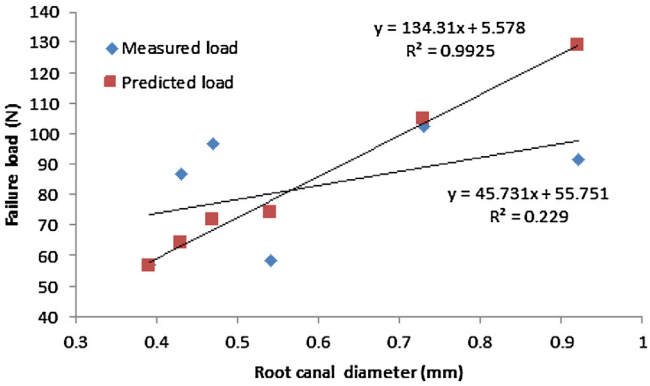


**Fig. 2 – Experimental and FEA-predicted failure loads based on a 75-MPa fracture strength vs root canal diameter.**

that equaled the applied load was obtained, was constrained in the vertical direction. The hoop or circumferential stress at the root canal surface was assumed to be the fracture-causing stress. It was determined as a function of the applied load.

## 3. Results

Table 2 summarizes the failure loads for the root sections. For the same taper, an increased root canal diameter did not lead to a reduced failure load. In fact, when the failure load was plotted against the root canal diameter for all the root sections, there appeared to be a positive, albeit weak, correlation between the two variables (Fig. 2).

The hoop or circumferential stress in the root section predicted by FEA is presented in Fig. 3. Its value is maximum at the enlarged root canal surface and reduces with increasing radial distance from the center. Its value is not fully uniform along the specimen's 2-mm thickness either, with it being lowest at the top surface and highest at the bottom surface (Fig. 4). The higher the load, the more nonlinear is the stress distribution along the vertical axis.

Tables 3–5 give the predicted failure loads of the root sections based on different failure stresses. Obviously, the higher the failure stress assumed, the higher the predicted failure load. Also, if the average, instead of the maximum, hoop stress at the root canal surface is used, the predicted failure

**Table 1 – Materials properties used for the finite-element model [34–36].**

| Material | Elastic modulus (GPa) | Poisson's ratio ($\nu$) | Reference |
|---|---|---|---|
| Steel base | 210 | 0.30 | Lanza et al., 2005 |
| Dentin | 18.6 | 0.31 | Peyton et al., 1952 |
| Stainless steel rod | 200 | 0.30 | Dieter, 2013 |

**Table 2 – Dimensions and failure loads of 2-mm thick root sections.**

| Group | Instrument taper | Distance from apex (mm) | Root canal diameter (mm) | Failure load (N) |
|---|---|---|---|---|
| 1 | 0.02 | 2-4 | 0.39 | 57.0 |
| 2 | 0.02 | 9.5-11.5 | 0.54 | 58.7 |
| 3 | 0.04 | 2-4 | 0.43 | 87.1 |
| 4 | 0.04 | 9.5-11.5 | 0.73 | 102.6 |
| 5 | 0.06 | 2-4 | 0.47 | 96.7 |
| 6 | 0.06 | 9.5-11.5 | 0.92 | 91.5 |

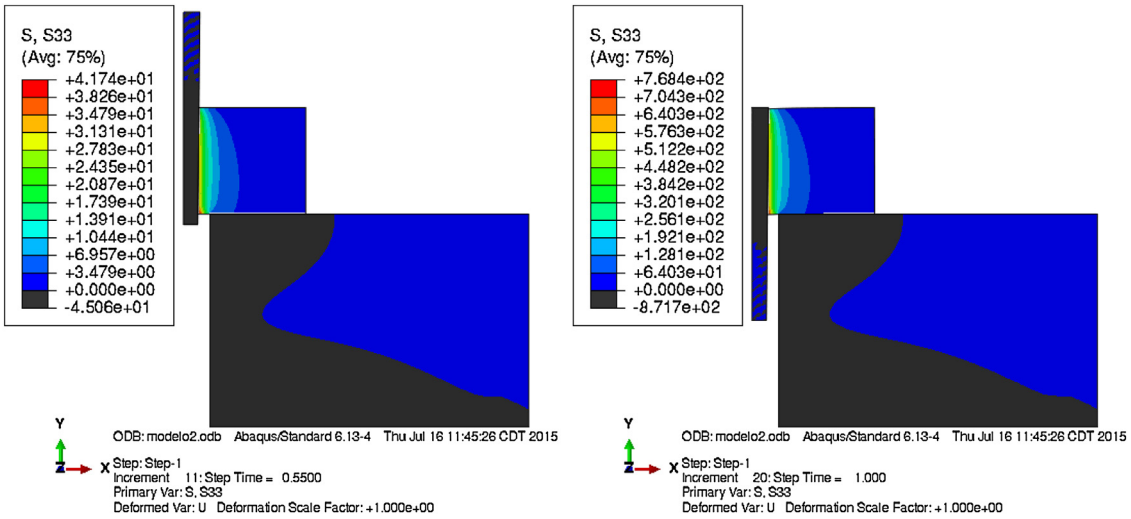


**Fig. 3 – Hoop stress (MPa) distribution in a root section (Group 2) at the beginning and end of loading.**

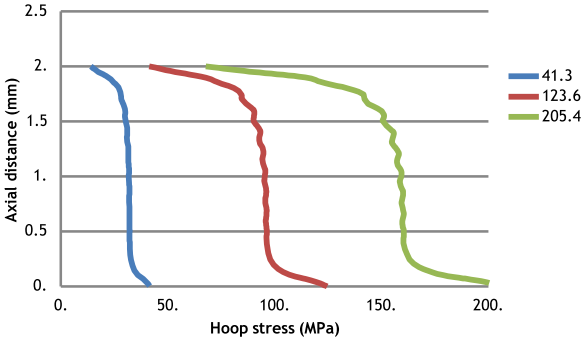


**Fig. 4 – Distribution of hoop stress at the root canal surface along the axial distance at different load levels (N).**

**Table 3 – Predicted failure load (N) based on a failure stress of 75 MPa.**

| Model | Experiment | Average | Maximum |
|---|---|---|---|
| 1 | 57 | 74.2 | 56.6 |
| 2 | 58.7 | 98.8 | 74.3 |
| 3 | 87 | 90.2 | 64.2 |
| 4 | 102.6 | 136.1 | 104.8 |
| 5 | 96.7 | 98 | 71.9 |
| 6 | 91.5 | 168.9 | 128.8 |
| Mean absolute difference | | 28.7 | 17.2 |

**Table 4 – Predicted failure load (N) based on a failure stress of 50 MPa.**

| Model | Experiment | Average | Maximum |
|---|---|---|---|
| 1 | 57 | 50.5 | 37.7 |
| 2 | 58.7 | 65.8 | 49.5 |
| 3 | 87 | 60.1 | 42.8 |
| 4 | 102.6 | 90.7 | 69.9 |
| 5 | 96.7 | 65.3 | 47.9 |
| 6 | 91.5 | 112.6 | 85.8 |
| Mean absolute difference | | 55.6 | 26.6 |

**Table 5 – Predicted failure load (N) based on a failure stress of 40 MPa.**

| Model | Experiment | Average | Maximum |
|---|---|---|---|
| 1 | 57 | 40.4 | 30.2 |
| 2 | 58.7 | 52.7 | 39.6 |
| 3 | 87 | 48.1 | 34.2 |
| 4 | 102.6 | 72.6 | 55.9 |
| 5 | 96.7 | 52.2 | 38.3 |
| 6 | 91.5 | 90 | 68.7 |
| Mean absolute difference | | 22.9 | 37.7 |

load would also be higher. Tables 3–5 also provide the mean absolute difference between the predicted and the measured failure loads. It can be seen that predictions based on the maximum hoop stress and a failure stress of 75 MPa are closest to the experimental values. Further, when the predicted failure load is plotted against the root canal diameter, a clear positive linear relationship can be seen (Fig. 2).

## 4. Discussion

Perhaps counterintuitively, both the experimental and numerical results indicated that the fracture

load increased with increasing root canal diameter. To help explain these results, we derive below an expression for the critical load required to fracture the root section with a rod using simple principles of mechanics. Fig. 5 shows the relevant parameters considered in the derivation. Their definitions are given as follows:

With reference to Fig. 5, the balance of forces for either the rod or root section in the vertical and horizontal directions was considered. Vertically,

$$Q = (F \cos\theta + R \sin\theta) \times \pi D t. \quad (1)$$

Horizontally, the reaction and friction forces combine to produce a pressure on the inner wall of the

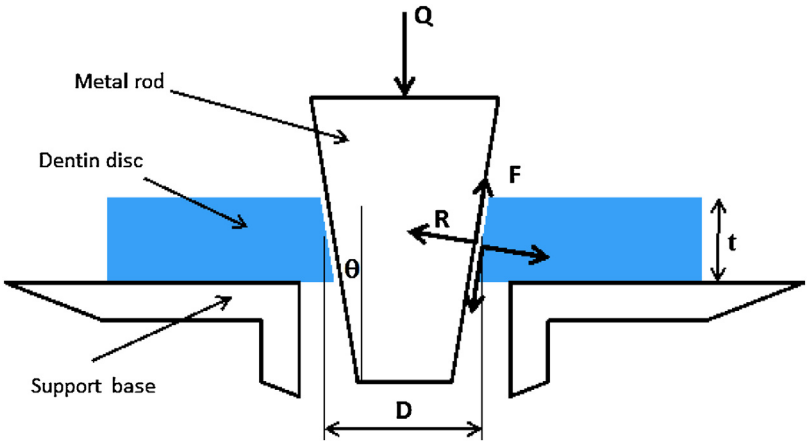


**Fig. 5 – Forces between insertion rod and root dentin section.**

root section of

$$p = -F \sin\theta + R\cos\theta. \quad (2)$$

Now, the frictional force and the reaction force is related via $F = \mu R$. Therefore,

$$Q = R(\mu \cos\theta + \sin\theta) \times \pi Dt, \quad (3)$$

and

$$p = R(-\mu \sin\theta + \cos\theta). \quad (4)$$

Dividing equation (3) by (4) gives:

$$\frac{Q}{\pi Dtp} = \frac{\mu \cos\theta + \sin\theta}{-\mu \sin\theta + \cos\theta}$$

or

$$Q = \pi Dtp \frac{\mu + \tan\theta}{1 - \mu \tan\theta}. \quad (5)$$

According to Pilkey and Pilkey [37], the maximum hoop stress in the root section is related to the internal pressure via:

$$\sigma_{max} = kp = \frac{kQ}{\pi Dt}\left(\frac{1 - \mu \tan\theta}{\mu + \tan\theta}\right), \quad (6)$$

where $k$ is the stress concentration factor, which depends on the ratio between the root canal diameter and the planar dimensions of the root section. Hence, at fracture, i.e. when $\sigma_{max}$ is equal to the fracture strength of dentin ($\delta\delta_{ff}$), the vertical force reaches its critical value of:

$$Q_f = \pi Dt\left(\frac{\sigma_f}{k}\right)\frac{\mu + \tan\theta}{1 - \mu \tan\theta}. \quad (7)$$

When the root canal diameter is much smaller than the planar dimensions of the root section, kk≈ 1.

Fig. 6 compares the maximum hoop stress at the root canal surface as predicted by Equation (6) with the corresponding average and maximum hoop stress predicted by FEA. As can be seen, the analytical solution lies in between the two sets

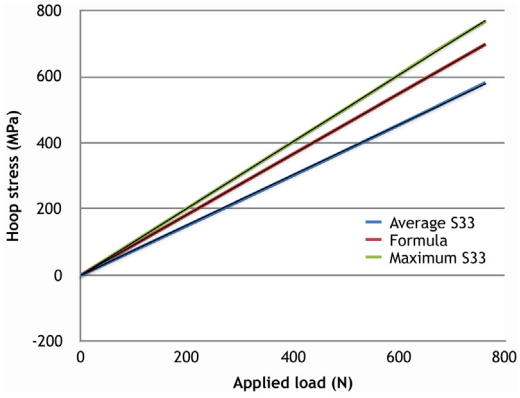


**Fig. 6 – Hoop stresses at root canal surface as functions of applied load predicted by FEA and analytical solution for Model 2.**

of numerical results, demonstrating its validity. The predicted fracture loads based on the analytical solution are therefore expected to be similar to those given by the FEA (Fig. 2).

In practice, there is bending of the root section during its loading by the rod, giving rise to compression at the top surface and tension at the bottom surface. The superimposition of these bending stresses to those induced by the expansion of the root canal results in the nonuniform stress distributions at the root canal surface seen in Figs. 3 and 4.

Equation (7) shows that the fracture load of a root section is proportional to its root canal diameter, which agrees with the FEA and, to a lesser extent, the experimental results found in this study. It also shows that the fracture load increases with the taper. Both of these theoretical predictions agree with the findings by Holcomb et al. [38] that the fracture load has positive linear correlations with canal width and canal taper. Intuitively, as the root canal diameter increases, there will be a bigger circumferential area to distribute the contact pressure, leading to lower fracture-causing stresses.

The difference between the experimental and predicted fracture loads was probably caused by errors in the fracture strength assumed and the possible anisotropic behavior of dentin, which was not considered in the FEA. The weak linear

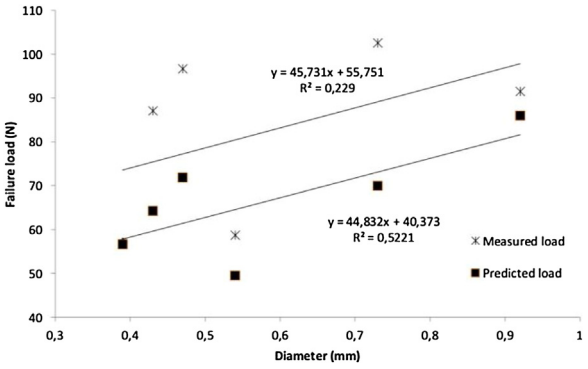


**Fig. 7 – Experimental and FEA-predicted failure loads based on variable fracture strength vs. root canal diameter.**

correlation between fracture load and root canal diameter was attributed to the variation in fracture strength of root dentin along the axial position. Indeed, Mannocci et al. [39] showed that the tensile strength of middle-apical dentin was significantly higher than that of coronal dentin. If we use 75 MPa and 50 MPa as the fracture strength of apical and coronal dentin, respectively, for our predictions, the correlation between the predicted failure load and root canal diameter would be very similar to that for the experimental values, albeit with a systematic error; see Fig. 7.It should be pointed out that thin root dentin sections are limited in their representation of the actual clinical situation. Things are more complicated in whole teeth, for which 3D FEA will definitely be required. According to Lertchirakarn et al. [26], VRFs are not the direct result of hoop stresses uniformly distributed around the canal but from asymmetrical stress concentration. When the canal shape or the external root cross-sectional shape is not circular, the stress distribution becomes asymmetrical. Also, when the root dentin wall thickness was reduced in one direction, stress distribution would also not be uniform. Reducing the radius of curvature of the inner (canal) wall or outer root surface resulted in an increased tensile stress on the inner wall, in the same location as the reduced radius of curvature [22]. Thus, caution must be taken when using thin root sections to investigate the effect of endodontic instruments on vertical root fracture.

## 5. Conclusions

- For the same failure stress, the load required to cause fracture of the root dentin sections increases with the enlarged canal's taper and diameter, provided the latter is small compared to the overall dimensions of the section.
- In determining the maximum load allowed for root canal instrumentation, one must take into account differences in the fracture stress of dentin along the axial distance of the root.

## Acknowledgments

This work was supported by the Minnesota Dental Research Center for Biomaterials and Biomechanics and was carried out in part using the computer resources at the University of Minnesota Supercomputing Institute. Lais Munari received a scholarship from *Conselho de Aperfeiçoamento de Pessoal de Nível Superior* (CAPES#99999.006549/2014-04) and Alex Fok received a grant from National Natural Science Foundation of China (no. 81628005) in support of this work.

## REFERENCES

[1] Adorno CG, Yoshioka T, Suda H. The effect of working length and root canal preparation technique on crack development in the apical root canal wall. Int Endod J 2010;43:321–7.
[2] Scheafer E, Lau R. Comparison of cutting efficiency and instrumentation of curved canals with nickel-titanium and stainless-steel instruments. J Endod 1999;25:427–30.
[3] Vaudt J, Bitter K, Neumann K, Kielbassa AM. Ex vivo study on root canal instrumentation of two rotary nickel-titanium systems in comparison to stainless steel hand instruments. Int Endod J 2009;42:22–33.
[4] Arslan H, Barutcigil C, Karatas E, Topcuoglu HS, Yeter KY, Ersoy I, Ayrancı LB. Effect of citric acid irrigation on the fracture resistance of endodontically treated roots. Eur J Dent 2014;8:74–8.
[5] Usman N, Baumgartner JC, Marshall JG. Influence of instrument size on root canal debridement. J Endod 2004;30:110–2.
[6] Bier CA, Shemesh H, Tanomaru-Filho M, et al. The ability of different nickel-titanium rotary instruments to induce dentinal damage during canal preparation. J Endod 2009;35:236–8.
[7] Shemesh H, Bier CA, Wu MK, et al. Thee effects of canal preparation and filling on the incidence of dentinal defects. Int Endod J 2009;42:208–13.
[8] Shemesh H, Wesselink PR, Wu MK. Incidence of dentinal defects after root canal filling procedures. Int Endod J 2010;43:995–1000.
[9] Tamse A, Fuss Z, Lustig J, Kaplavi J. An evaluation of endodontically treated vertically fractured teeth. J Endod 1999;25:506–8.
[10] Capar ID, Arslan H, Akcay M, Uysal B. Effects of ProTaper Universal, ProTaper Next, and HyFlex instruments on crack formation in dentin. J Endod 2014;40:1482–4.
[11] Lam P, Palamara J, Messer H. Fracture strength of tooth roots following canal preparation by hand and rotary instrumentation. J Endod 2005;31:529–32.
[12] Pitts DL, Natkin E. Diagnosis and treatment to vertical root fractures. J Endod 1983;19:338–46.
[13] Gher ME, Dunlap RM, Anderson MH, Kuhl LV. Clinical survey of fractured teeth. J Am Dent Assoc 1987;114:174–7.
[14] Kim SY, Kim SH, Cho SB, Cho SB, Lee GO, Yang SE. Different treatment protocols for different pulpal and periapical diagnoses of 72 cracked teeth. J Endod 2013;39:449–52.
[15] Dang DA, Walton RE. Vertical root fracture and root distortion effects of spreader. J Endod 1989;15:294–301.
[16] Schwarz S, Lohbauer U, Petschelt A, et al. Vertical root fractures in crowned teeth: a report of 32 cases. Quintessence Int 2012;43:37–43.
[17] Meister F, Lommel TJ, Gerstein H. Diagnosis and possible causes of vertical root fractures. Oral Surg Oral Med Oral Path 1980;49:243–53.
[18] Barreto MS, Moraes RA, Rosa RA, et al. Vertical root fractures and dentin defects: effects of root canal preparation, filling, and mechanical cycling. J Endod 2012;38:1135–9.
[19] Cohen S, Blanco L, Berman L. Vertical root fractures: clinical and radiographic diagnosis. J Am Dent Assoc 2003;134:434–41.

[20] Pitts DL, Natkin E. Diagnosis and treatment of vertical root fractures. J Endod 1983;9(338):346.
[21] Abdo SB, Darrat AA, Masaudi SM, Luddin N, Husien A, Khamis MF. Comparison of over flared root canals of mandibular premolars filled with MTA and resin based material: An in vitro study. Smile Dent J 2012;7:38–42.
[22] Ricks-Williamson LJ, Fotos PG, Goel VK, Spivey JD, Rivera EM, Khera SC. A three- dimensional finite-element stress analysis of an endodontically prepared maxillary central incisor. J Endod 1995;21:362–7.
[23] Wilcox LR, Roskelley C, Sutton T. The relationship of root canal enlargement to finger- spreader induced vertical root fracture. J Endod 1997;23:533–4.
[24] Sathorn C, Palamara JE, Palamara D, Messer HH. Effect of root canal size and external root surface morphology on fracture susceptibility and pattern: A finite element analysis. J Endod 2005;31:288–92.
[25] Lertchirakarn V, Palamara JE, Messer HH. Patterns of vertical root fracture: Factors affecting stress distribution in the root canal. J Endod 2003;29:523–8.
[26] Lertchirakarn V, Palamara JE, Messer HH. Finite element analysis and strain-gauge studies of vertical root fracture. J Endod 2003;29:529–34.
[27] Sathorn C, Palamara JEA, Messer HH. A comparison of the effects of two canal preparation techniques on root fracture susceptibility and fracture pattern. J Endod 2005;31: 283–7.
[28] Ossareh A, Rosentritt M, Kishen A. Biomechanical studies on the effect of iatrogenic dentin removal on vertical root fractures. J Conserv Dent 2018;21(May-Jun (3)):290–6.
[29] Ikram OH, Patel S, Sauro S, Mannocci F. Micro-computed tomography of tooth tissue volume changes following endodontic procedures and post space preparation. Int Endod J 2009;42:1071–6.
[30] Pilo R, Shapenco E, Lewinstein I. Residual dentin thickness in bifurcated maxillary first premolars after root canal and post space preparation with parallel-sided drills. J Prosthet Dent 2008;99:267–73.
[31] Kalburge V, Yakub SS, Kalburge J, Hiremath H, Chandurkar A. A comparative evaluation of fracture resistance of endodontically treated teeth, with variable marginal ridge thicknesses, restored with composite resin and composite resin reinforced with ribbond: An in vitro study. Indian J Dent Res 2013;24:193–8.
[32] Mireku AS, Romberg E, Fouad AF, Arola D. Vertical fracture of root filled teeth restored with posts: The effects of patient age and dentine thickness. Int Endod J 2010;43:218–25.
[33] Zhou SR, Yu HY, Zheng J, Qian LM, Yan Y. Dental Biotribology. New York: Springer; 2013.
[34] Peyton FA, Mahler DB, Hershenov B. Physical properties of dentin. Journal of Dental Research 1952;31:366–70.
[35] Lanza A, Aversa R, Rengo S, Apicella D, Apicella A. 3D FEA of cemented steel, glass and carbon posts in a maxillary incisor. Dental Materials 2005;21:709–15.
[36] Dieter GE. Mechanical metallurgy. McGraw-Hill Book Company Inc; 2013.
[37] Pilkey WD, Pilkey DF. Peterson's Stress Concentration Factors. Jonh Wiley & Sons Inc; 2008.
[38] Holcomb Q, Pitts DL, Nicholls JI. Further investigation of spreader loads required to cause vertical root fracture during lateral condensation. J Endod 1987;13:277–84.
[39] Mannocci F, Pilecki P, Bertelli E, Watson TF. Density of dentinal tubules affects the tensile strength of root dentin. Dental Materials 2004;20:293–6.